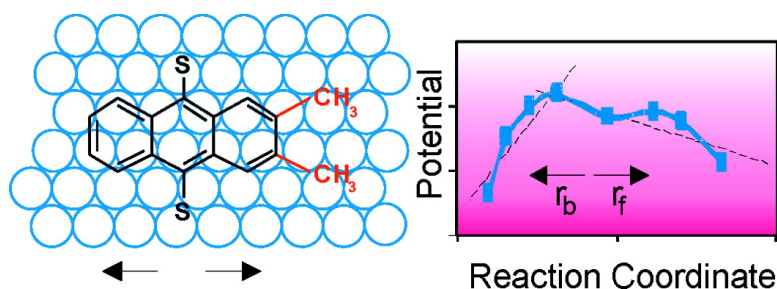


## Surface Diffusive Motion in a Periodic and Asymmetric Potential

Greg Pawin, Kin L. Wong, Ki-Young Kwon, Robert J. Frisbee, Talat S. Rahman, and Ludwig Bartels

*J. Am. Chem. Soc.*, **2008**, 130 (46), 15244-15245 • DOI: 10.1021/ja8064039 • Publication Date (Web): 28 October 2008

Downloaded from <http://pubs.acs.org> on February 8, 2009



### More About This Article

Additional resources and features associated with this article are available within the HTML version:

- Supporting Information
- Access to high resolution figures
- Links to articles and content related to this article
- Copyright permission to reproduce figures and/or text from this article

[View the Full Text HTML](#)

## Surface Diffusive Motion in a Periodic and Asymmetric Potential

Greg Pawin,<sup>†</sup> Kin L. Wong,<sup>†</sup> Ki-Young Kwon,<sup>†</sup> Robert J. Frisbee,<sup>†</sup> Talat S. Rahman,<sup>\*,‡</sup> and Ludwig Bartels<sup>\*,†</sup>

Pierce Hall, University of California, Riverside, California 92521, and Department of Physics, University of Central Florida, Orlando, Florida 32816

Received August 12, 2008; E-mail: talat@physics.ucf.edu; Ludwig.Bartels@ucr.edu

Controlling the behavior of molecules at surfaces has become a research topic of significant interest, not the least because of the appeal of molecular machines as examples of ultimate miniaturization of macroscopic devices. Behaviors such as in-plane rotation,<sup>1,2</sup> normal rotation,<sup>3</sup> bipedal locomotion,<sup>4,5</sup> and sky-hooks<sup>6</sup> have been described, and resemblances to macroscopic devices such as gears,<sup>1</sup> cars,<sup>7</sup> ratchets,<sup>8</sup> turnstiles,<sup>9</sup> shuttles,<sup>10</sup> etc. have been highlighted.<sup>11</sup> Also the biochemical arena features many molecules that were likened to macroscopic mechanical devices (F1-motor of ATP synthase, proton pump in cell membranes, transcription polymerase, kinesin motor proteins). Further progress in man-made surface molecular devices requires an understanding of how small chemical modifications impact properties of molecular surface motion such as diffusion rate, prefactor, and symmetry. In this quest, this manuscript presents how simple methylation of a molecule far from the fulcrum of its substrate interaction can dramatically affect its diffusive properties: for 9,10-dithioanthracene (DTA)<sup>4</sup> we observe an  $\sim 100$ -fold decrease in surface mobility caused by an  $\sim 2$ -fold increase of the diffusion barrier. Despite these significant ramifications of the unilateral distortion of the DTA potential energy landscape, the overall symmetry of DTA diffusion<sup>4</sup> is not affected, highlighting the applicability of the Principle of Microscopic Reversibility to single molecular motion, i.e. beyond the ensemble averages probed in conventional chemical experiments.<sup>8</sup>

Surface diffusion of many small species (e.g., metal atoms, CO molecules) has been studied in detail with a focus on their impact on epitaxy or heterogeneous catalysis; fundamental and systematic exploration of the diffusive characteristics of larger molecules are, with a few exceptions including refs 3 and 12, not yet available. Recently we reported<sup>4</sup> on the particular property of DTA (Figure 1) to diffuse in a uniaxial fashion on isotropic Cu(111): upon adsorption, DTA aligns its aromatic backbone with one of the three equivalent substrate atomic rows ( $\{110\}$  directions) and then diffuses exclusively along this row, i.e. avoiding at each step four out of six equivalent nearest neighbor adpositions and thereby violating the substrate symmetry. The adsorption ground state of DTA/Cu(111) has a mirror plane at the center of the molecule and normal to the diffusion direction, which renders diffusion “forward” and “backward” equivalent. Here we explore how asymmetric methylation impacts its diffusive behavior.

The synthesis of 2,3-dimethyl-9,10-dithioacetylthranthracene is outlined in the Supporting Information (SI). A clean coverage of DMDTA of one molecule per 1000 substrate atoms is prepared by a sequence of vacuum evaporation onto a sputter-and-anneal cleaned Cu(111) sample held at liquid nitrogen temperatures and removal of the protection groups through annealing to room temperature. Variable temperature scanning tunneling microscopy (STM) reveals DMDTA as an oblong feature with two faint shoulders on the sides and a pronounced protrusion at one end (Figure 1). Comparison to images of DTA<sup>4</sup> shows that the lateral shoulders represent the thiol linkers and the terminal protrusion the methyl-substituted end of the molecule.



**Figure 1.** DMDTA (left) appears in STM ( $65 \times 30 \text{ \AA}$ , 1.4 V, 60 pA) with its long anthracene moiety and a unilateral protrusion reflecting the methyl substitution. For comparison, the insert shows an STM image of DTA.

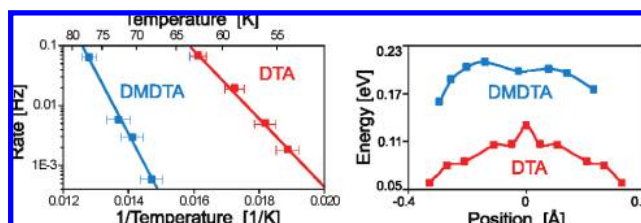


**Figure 2.** (Left) Arrhenius plot of DTA and DMDTA diffusion. Vertical error bars are smaller than the symbols, and horizontal bars correspond to 1 K uncertainty in the temperature calibration. The barriers and prefactors are 0.13 eV,  $4 \times 10^9$  and 0.21 eV,  $2 \times 10^{12}$ , respectively. (Right) DFT-based simulation of the diffusion barriers for DTA and DMDTA in the vicinity of the diffusion midpoint (zero on x-axis). The average distance of the sulfur atoms from the high-symmetry DTA transition state was used as reaction coordinate.

Acquisition of thousands of consecutive STM images shows that DMDTA exhibits the same uniaxial diffusion as DTA, yet it diffuses  $\sim 1000$  times slower than DTA, despite the inert nature of the methyl substitution, the substitution’s remoteness from the fulcrum of the molecule–substrate interaction, and the small mass difference of the molecules ( $\sim 5\%$ ). Temperature dependent measurements of the diffusion rates result in the Arrhenius plot of Figure 2. It shows a significant impact of the asymmetric methyl substitution on both the diffusion prefactor ( $\sim 1:500$ ) and barrier height ( $\sim 1:2$ ).

We performed density functional theory (DFT) calculations comparing DTA and DMDTA on a supercell of  $6 \times 6$  substrate atoms in three layers (total 108 atoms), sufficiently large to model the dynamics of both molecules. A side view of the cumulative charge density for (DM)DTA in the ground state is shown in Figure 3a,b. The aromatic ring system of DTA is V-shaped with the outer rings pointing away from the Cu substrate, an affect originally attributed to the strong pull toward the substrate exerted by the central S atoms. The two additional methyl groups of DMDTA render the V-shape asymmetric by tilting the methyl side of the molecule up, partially at the expense of the opposite aromatic ring of the molecule as seen in the difference between the DTA and DMDTA charge densities (Figure 3c). The closer approach of the nonmethylated side of DMDTA, while not energetically favorable per se (as otherwise it would have been adopted by DTA as well), is bound to increase the interaction of this ring system with the substrate (i). The methyl groups appear as a hook at the side of the molecule, almost resembling the pawl of a ratchet, and cause significant perturbation of the substrate charge distribution underneath

<sup>†</sup> University of California.

<sup>‡</sup> University of Central Florida.

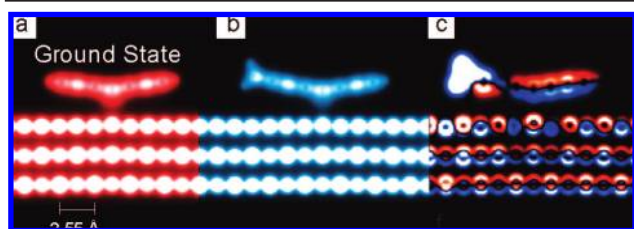


**Figure 3.** Simulated charge density at the ground state for DTA (a), DMDTA (b), and their difference (c) integrated over the depth of the molecule. Due to the antiphase nature of successive (110) atomic rows on Cu(111), the substrate atoms appear twice as closely spaced.

(ii). Observations (i) and (ii) provide a phenomenological explanation for the increase in diffusion barrier experienced by DMDTA.

We have also applied DFT calculations to compare the shape of the potential energy surface for DTA and DMDTA near the diffusion transition state; i.e. we calculated the total energy of supercells of DTA and DMDTA fixing the position of one of the two S atoms along the diffusion direction while relaxing all other degrees of freedom of the molecule and the substrate. The asymmetric methylation not only has an impact on the height of the barrier but also shifts it laterally: at DMDTA's transition state, its S atoms are still on average 0.1 Å to the side of symmetric DTA transition state and the molecule's aromatic moiety is at an angle of  $\sim 2^\circ$  to the diffusion direction.

A comparison of the calculated charge densities of DTA and DMDTA at the DTA transition state shows a larger impact of the molecule on the substrate geometry for DMDTA (see SI), a further indication of the stronger DMDTA–substrate interaction and higher diffusion barrier. The effect of the asymmetric substitution on the charge distribution and the diffusion rate/barrier/prefactor is very illustrative: diffusion prefactors contain information on vibrational entropic contributions which are naturally connected to the coupling between the system electronic structure and its vibrational dynamics. The increase of 3 orders of magnitude of the diffusion prefactor upon asymmetric substitution is most likely related to the softening of vibrational modes, as a result of differences in the substrate–adsorbate interactions in the two cases. Our observation of a correlated increase in diffusion barrier and diffusion prefactor is another manifestation of the compensation effect known as the Meyer–Neldel rule.<sup>13</sup>

The findings described so far show that even an inert substitution can have a substantial impact on the dynamics of a molecule at a metal surface. We found that the linear nature of the diffusive behavior of DTA is robust under methylation of the aromatic system, suggesting such molecular guidance may be applicable in a more general fashion. We now address the ramifications the asymmetric nature of the substitution and the diffusion barrier have on the symmetry of the diffusive behavior, i.e. on the branching ratio between movement in and counter to the direction of methylation. We treat the diffusion of (DM)DTA as a reversible chemical reaction similar to any transfer of a moiety X between two equivalent bonding partners A,A':  $AX + A' \rightarrow A + XA'$ .

In classical mechanics, at the base of any ratcheting motion is a sawtooth potential, i.e. a potential with different length  $ab$  of ascending and descending slope. The ratio  $a/b$  then defines the ratio of the forces required for backward and forward movement. If we apply this model to the dynamics of DMDTA, the offset of its transition state from the diffusion midpoint of 0.1 Å at a potential periodicity of 2.55 Å leads to a ratio of  $a/b$  of  $1.375 \text{ Å}/1.175 \text{ Å} = 1.17$ , i.e. a 17% preference for movement in one direction. This purely geometric approximation is, of course, subject to severe limitations, such as some degree of arbitrariness in the choice of the metric of the reaction coordinate and disregard for the actual, complex shape of the diffusion potential. Are

such geometric considerations, however, applicable at all given the microscopic and quantum nature of the system?

In 1924 Tolman postulated<sup>14</sup> that the rate of any chemical reaction in thermal equilibrium is identical in forward and backward directions and, thus, only dependent on the height and not on the shape of the barrier. Tolman's "Principle of Microscopic Reversibility"<sup>15</sup> and the concept of Detailed Balance have since become an undisputed foundation of modern chemistry. Their experimental testing at the single particle scale is not straightforward, however, and despite the reference to "Microscopic" in its name, the authors are not aware of any nonensemble measurement directly addressing it. Yet considerable theoretical and experimental effort still concerns the energetics of ensemble realizations of systems with asymmetric pathways.<sup>8,16</sup>

STM allows direct observation of the branching ratio between forward and backward diffusion of DMDTA; by evaluation of  $\sim 1300$  molecular movements, we find a forward/backward ratio of  $1.009 \pm 0.01$ , i.e. less than 1% deviation from unity. This is in stark contrast to the classical behavior described above but in perfect agreement with Tolman's prediction. These measurement resonate in their simplicity with his original reasoning, in which he (following Marcelin<sup>17</sup>) likened "Microscopic Reversibility" to the travel of people between two cities separated by a mountain.<sup>15</sup>

**Acknowledgment.** Supported by the DOE/DE-FGO2-03ER15464/07ER15842 and the NSF 0647152. Computational resources of the San Diego Supercomputer Center.

**Supporting Information Available:** Description of synthetic, experimental, and computational methods; movie of DMDTA motion. This material is available free of charge via the Internet at <http://pubs.acs.org>.

## References

- (1) Gimzewski, J. K.; Joachim, C.; Schlittler, R. R.; Langlais, V.; Tang, H.; Johansson, I. *Science* **1998**, *281*, 531–533.
- (2) Maksymovych, P.; Sorescu, D. C.; Dougherty, D.; Yates, J. T. *J. Phys. Chem. B* **2005**, *109*, 22463–22468.
- (3) Grill, L.; Rieder, K. H.; Moresco, F.; Rapenne, G.; Stojkovic, S.; Bouju, X.; Joachim, C. *Nat. Nanotechnol.* **2007**, *2*, 95–98. Martinsinovich, N.; Hobbs, C.; Kantorovich, L.; Fawcett, R. H. J.; Humphry, M. J.; Keeling, D. L.; Beton, P. H. *Phys. Rev. B* **2006**, *74*, 085304.
- (4) Kwon, K. Y.; Wong, K. L.; Pawin, G.; Bartels, L.; Stolbov, S.; Rahman, T. S. *Phys. Rev. Lett.* **2005**, *95*, 166101.
- (5) Wong, K. L.; Pawin, G.; Kwon, K. Y.; Lin, X.; Jiao, T.; Fawcett, R.; Solanki, U.; Bartels, L.; Stolbov, S.; Rahman, T. S. *Science* **2007**, *315*, 1391–1393.
- (6) Horch, S.; Lorensen, H.; Helveg, S.; Laegsgaard, E.; Stensgaard, I.; Jacobsen, K.; Norskov, J.; Besenbacher, F. *Nature* **1999**, *398*, 134–136.
- (7) Shirai, Y.; Osgood, A. J.; Zhao, Y. M.; Kelly, K. F.; Tour, J. M. *Nano Lett.* **2005**, *5*, 2330–2334.
- (8) Kelly, T. R.; De Silva, H.; Silva, R. A. *Nature* **1999**, *401*, 150–152.
- (9) Moore, J. S. *Acc. Chem. Res.* **1997**, *30*, 402–413.
- (10) Balzani, V.; Credi, A.; Raymo, F. M.; Stoddart, J. F. *Angew. Chem., Int. Ed.* **2000**, *39*, 3348–3391.
- (11) Kottas, G. S.; Clarke, L. I.; Horinek, D.; Michl, J. *Chem. Rev.* **2005**, *105*, 1281–1376. van Delden, R. A.; ter Wiel, M. K. J.; Pollard, M. M.; Vicario, J.; Koumura, N.; Feringa, B. L. *Nature* **2005**, *437*, 1337–1340. Kay, E. R.; Leigh, D. A.; Zerbetto, F. *Angew. Chem.* **2007**, *46*, 72–191. Liu, Y.; Flood, A. H.; Bonvallet, P. A.; Vignon, S. A.; Northrop, B. H.; Tseng, H. R.; Jeppesen, J. O.; Huang, T. J.; Brough, B.; Baller, M.; Magonov, S.; Solares, S. D.; Goddard, W. A.; Ho, C. M.; Stoddart, J. F. *J. Am. Chem. Soc.* **2005**, *127*, 9745–9759.
- (12) Otero, R.; Hummelink, F.; Sato, F.; Legoas, S. B.; Thstrup, P.; Laegsgaard, E.; Stensgaard, I.; Galvao, D. S.; Besenbacher, F. *Nat. Mater.* **2004**, *3*, 779–782. Shirai, Y.; Osgood, A. J.; Zhao, Y. M.; Yao, Y. X.; Saudan, L.; Yang, H. B.; Chiu, Y. H.; Alemany, L. B.; Sasaki, T.; Morin, J. F.; Guerrero, J. M.; Kelly, K. F.; Tour, J. M. *J. Am. Chem. Soc.* **2006**, *128*, 4854–4864.
- (13) Meyer, W.; Neldel, H. *Phys. Z.* **1937**, *38*, 1014–1019. Boisvert, G.; Lewis, L. J.; Yelon, A. *Phys. Rev. Lett.* **1995**, *75*, 469–472.
- (14) Tolman, R. C. *Phys. Rev.* **1924**, *23*, 693–709.
- (15) Tolman, R. C. *Proc. Natl. Acad. Sci. U.S.A.* **1925**, *11*, 436–439.
- (16) Astumian, R. D. *Proc. Natl. Acad. Sci. U.S.A.* **2007**, *104*, 19715–19718. Leigh, D. A.; Wong, J. K. Y.; Dehez, F.; Zerbetto, F. *Nature* **2003**, *424*, 174–179. Berry, M. *Physics Today* **1990**, *43*, 34–40.
- (17) Marcelin, R. *Ann. Phys.* **1915**, *3*, 173.

JA8064039